Supporting Information

Photo-assisted water oxidation by high-nuclearity cobalt-oxo cores: tracing the catalyst fate during oxygen evolution turnover

M. Natali,[a] I. Bazzan,[b] S. Goberna-Ferrón,[c] R. Al-Oweini,[b,d] M. Ibrahim,[d] B. Bassil,[d] H. Dau,[e] F. Scandola,[a] J. R. Galán-Mascarós,[c] U. Kortz,[d] A. Sartorel,[b] I. Zaharieva,[e] and M. Bonchio[b]

a) Department of Chemical and Pharmaceutical Sciences, University of Ferrara, Via Fossato di Mortara 17-19, and Centro Interuniversitario per la Conversione Chimica dell'Energia Solare (SolarChem), sez. di Ferrara, via L. Borsari 46, 44121 Ferrara, Italy.

b) Department of Chemical Sciences University of Padova and Institute on Membrane Technology, Unit of Padova, via F. Marzolo 1, 35131, Padova, Italy.

c) Institute of Chemical Research of Catalonia (ICIQ), The Barcelona Institute of Science and Technology (BIST), Av. Paisos Catalans, 16, E-43007, Tarragona (Spain) and ICREA, Passeig Lluis Companys, 23, E-08010, Barcelona (Spain).

d) Jacobs University, Department of Life Sciences and Chemistry, Campus Ring 1, 28759 Bremen (Germany).

e) Freie Universität Berlin, FB Physik, Arnimallee 14, 14195 Berlin, Germany.

Content **Page**

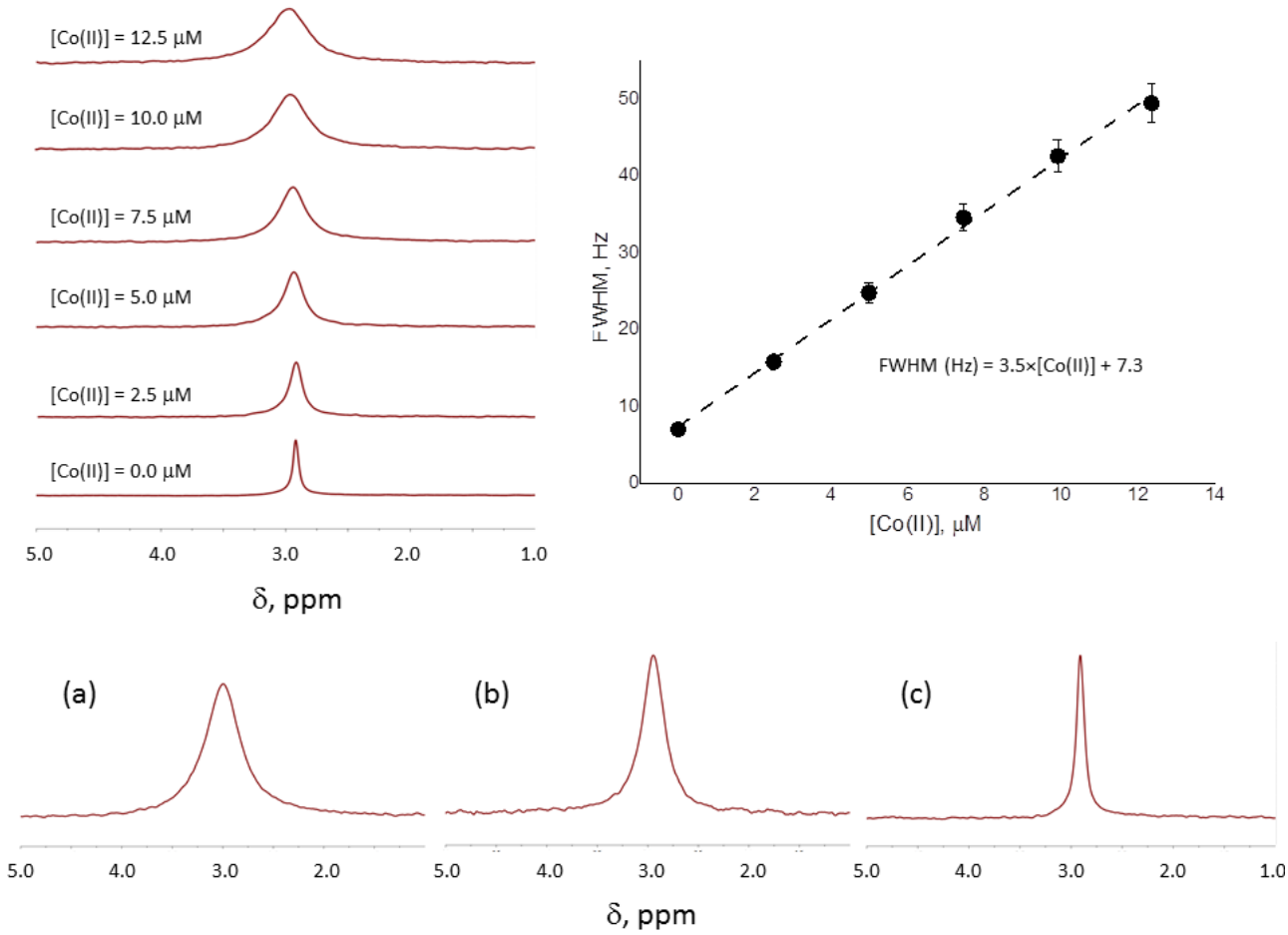

Figure S1. ^{31}P-NMR line broadening experiments in 20 mM phosphate buffer, pH 8 (with 10% D_2O). Top left: ^{31}P-NMR spectra in the presence of increasing concentrations of Co(II) aqua ions (0-12.5 µM, introduced as hexahydrate $Co(NO_3)_2$). Top right: calibration of Full Width at Half Maximum (FWHM) versus Co(II) concentration. Bottom: ^{31}P NMR spectra in 20 mM phosphate buffer, pH 8 (with 10% D_2O) of: (a) **Co_9**, 1 mM total Co concentration (FWHM = 49 Hz); (b) **Co_{15}**, 250 µM total Co concentration (FWHM = 31 Hz); (c) **Co_{16}**, 1 mM total Co concentration (FWHM = 12 Hz).

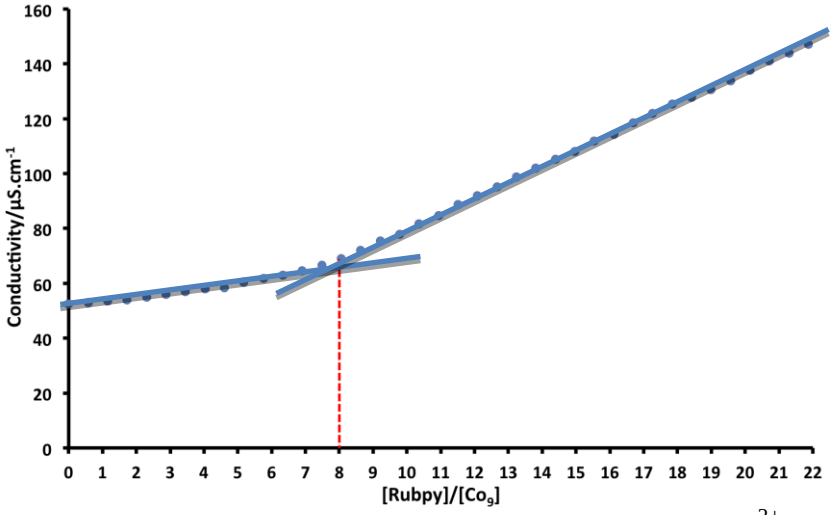

Figure S2. Conductometric titration of **Co_9** (34 µM in water) with $Ru(bpy)_3^{2+}$ (aliquots added from a 30 mM solution in water).

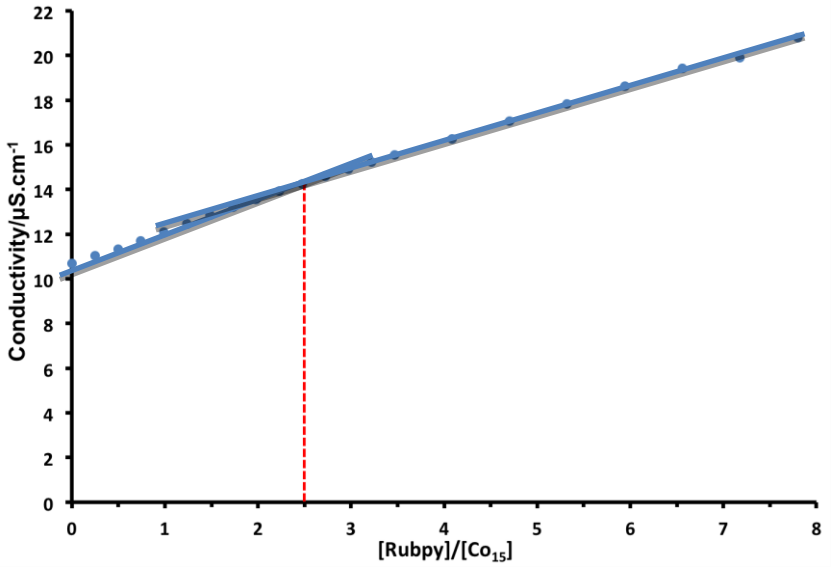

Figure S3. Conductometric titration of **Co_{15}** (8 µM in water) with $Ru(bpy)_3^{2+}$ (aliquots added from a 30 mM solution in water).

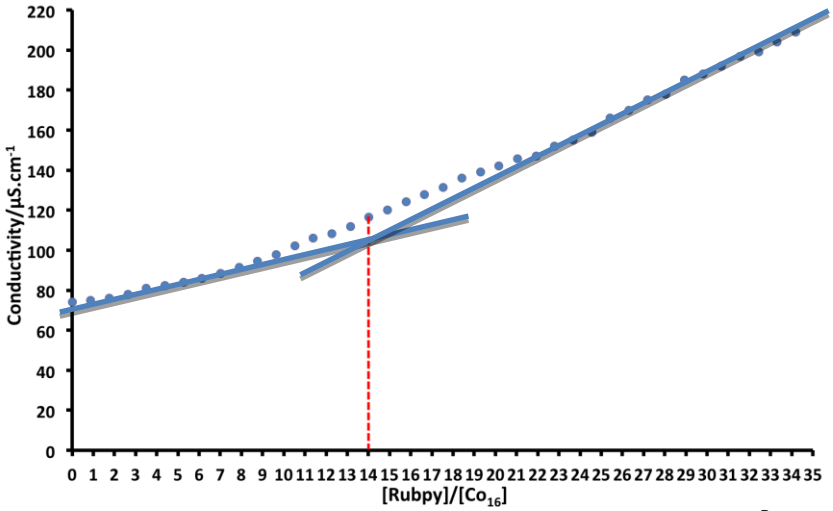

Figure S4. Conductometric titration of **Co_{16}** (21 µM in water) with $Ru(bpy)_3^{2+}$ (aliquots added from a 30 mM solution in water).

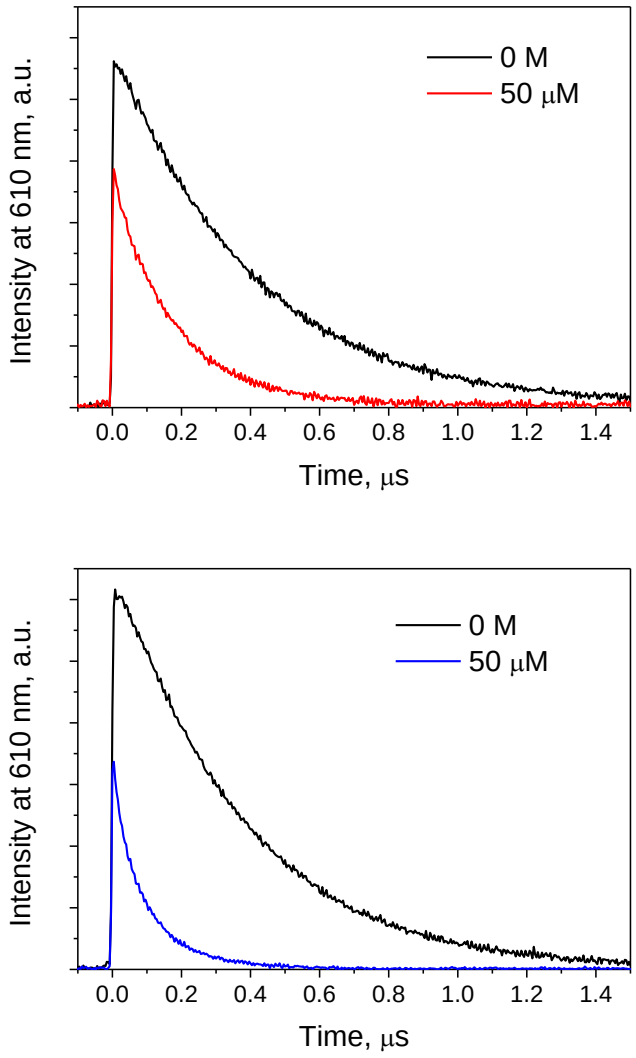

Figure S5. Time-resolved emission experiments (excitation at 355 nm, analysis at 610 nm) of $Ru(bpy)_3^{2+}$ (black traces) and $Ru(bpy)_3^{2+}$ with one equivalent of **Co_9** (top, red trace) and **Co_{16}** (bottom, blue trace).

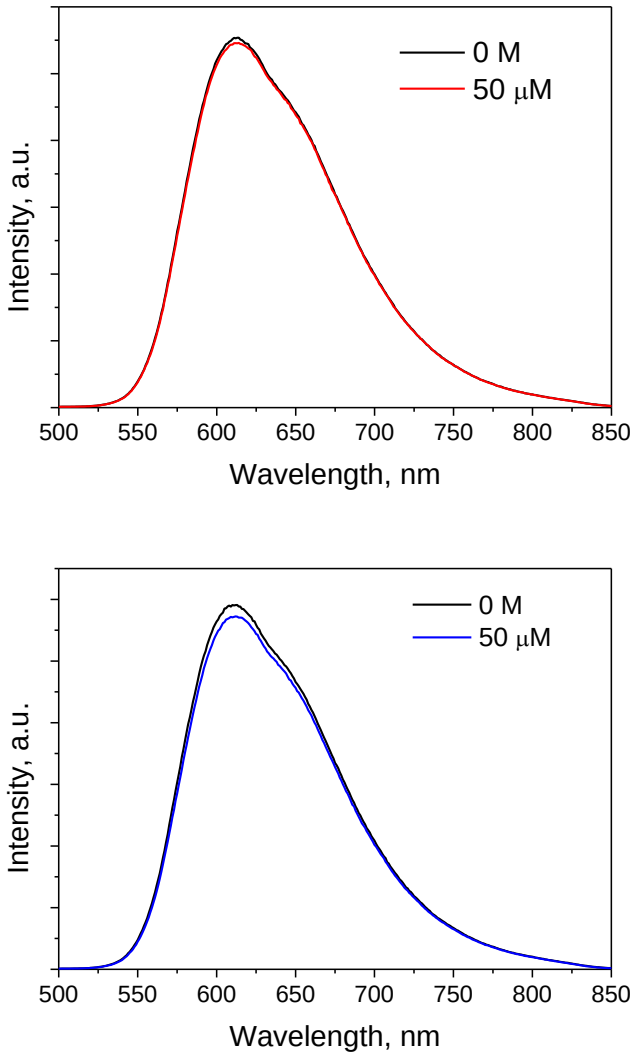

Figure S6. Emission experiments of $Ru(bpy)_3^{2+}$ (black traces) and $Ru(bpy)_3^{2+}$ with one equivalent of **Co_9** (red trace, top) and **Co_{16}** (blue trace, bottom) in 50 mM phosphate buffer, pH 8.

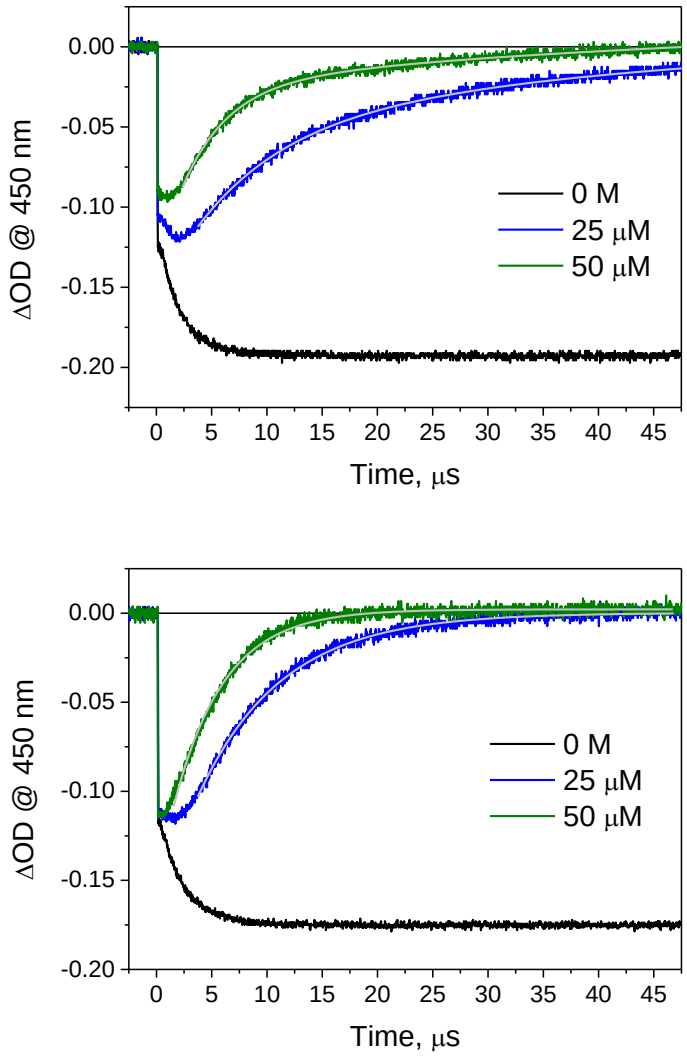

Figure S7. Laser flash photolysis experiments (λ_{exc} = 355 nm) in 50 mM phosphate buffer (pH 8) containing 5 mM $S_2O_8^{2-}$, 50 μM $Ru(bpy)_3^{2+}$ and 0-50 μM **Co$_{15}$** (top) or 0-50 μM **Co$_{16}$** (bottom).

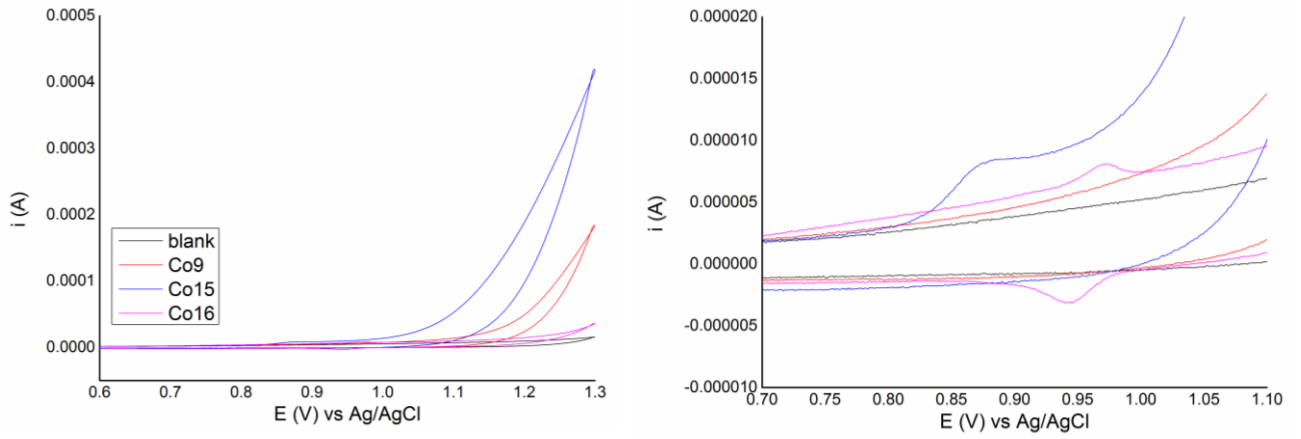

Figure S8. Cyclic voltammetry of Co-POMs in 0.1 M phosphate buffer, pH 8 (0.5 mM total cobalt concentration). Working electrode: glassy carbon, counter electrode: platinum, reference electrode: Ag/AgCl, scan rate: 0.1 Vs^{-1}.

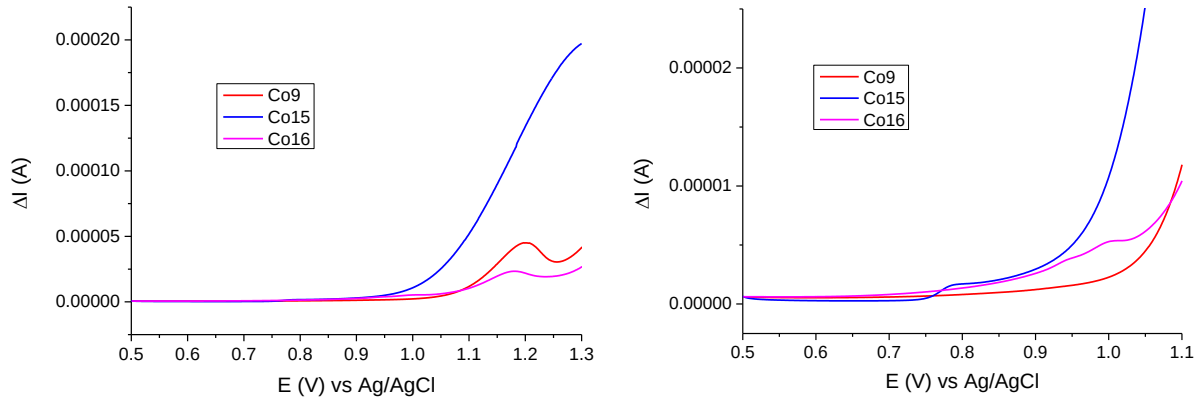

Figure S9. Square-wave voltammetry (SWV) of Co-POMs in 0.1 M phosphate buffer, pH 8 (0.5 mM total cobalt concentration). Working electrode: glassy carbon, counter electrode: platinum, reference electrode: Ag/AgCl, scan rate: 0.01 Vs^{-1}, ΔE = 50 mV.

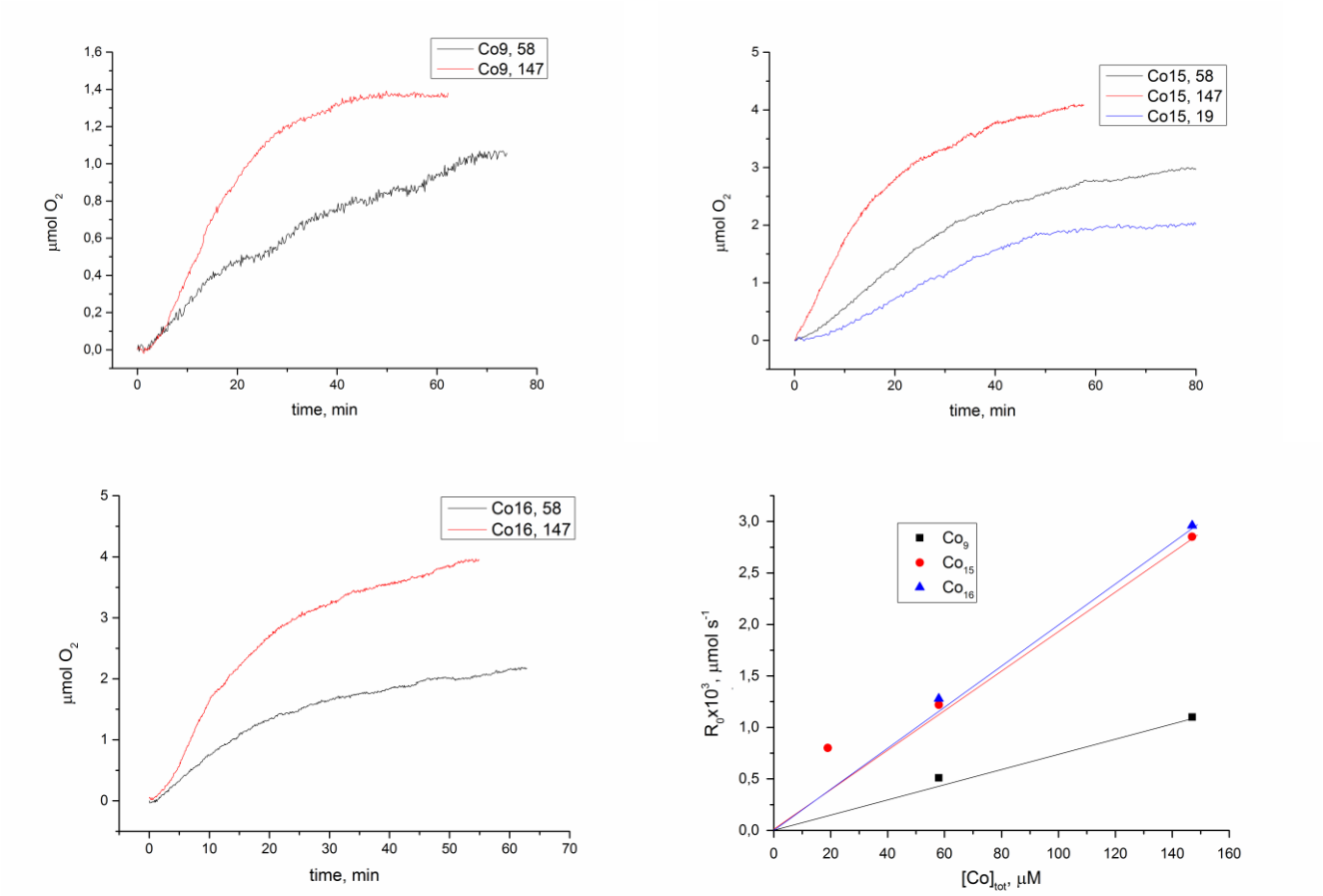

Figure S10. O_2 production kinetics from 15 ml of a 20 mM phosphate buffered solution (pH 8) containing $Ru(bpy)_3^{2+}$ (1 mM), $S_2O_8^{2-}$ (5 mM) and **Co$_9$**, **Co$_{15}$** or **Co$_{16}$**. Irradiation with a tungsten lamp (cut-off filter at 375 nm, power density 90 mW·cm^{-2}). Top, left: **Co$_9$** with 58-147 µM total cobalt concentration; top, right: **Co$_{15}$** with 19-147 µM total cobalt concentration; bottom, left: **Co$_{16}$** with 58-147 µM total cobalt concentration; bottom, right: plot of the initial rates versus total cobalt concentration.

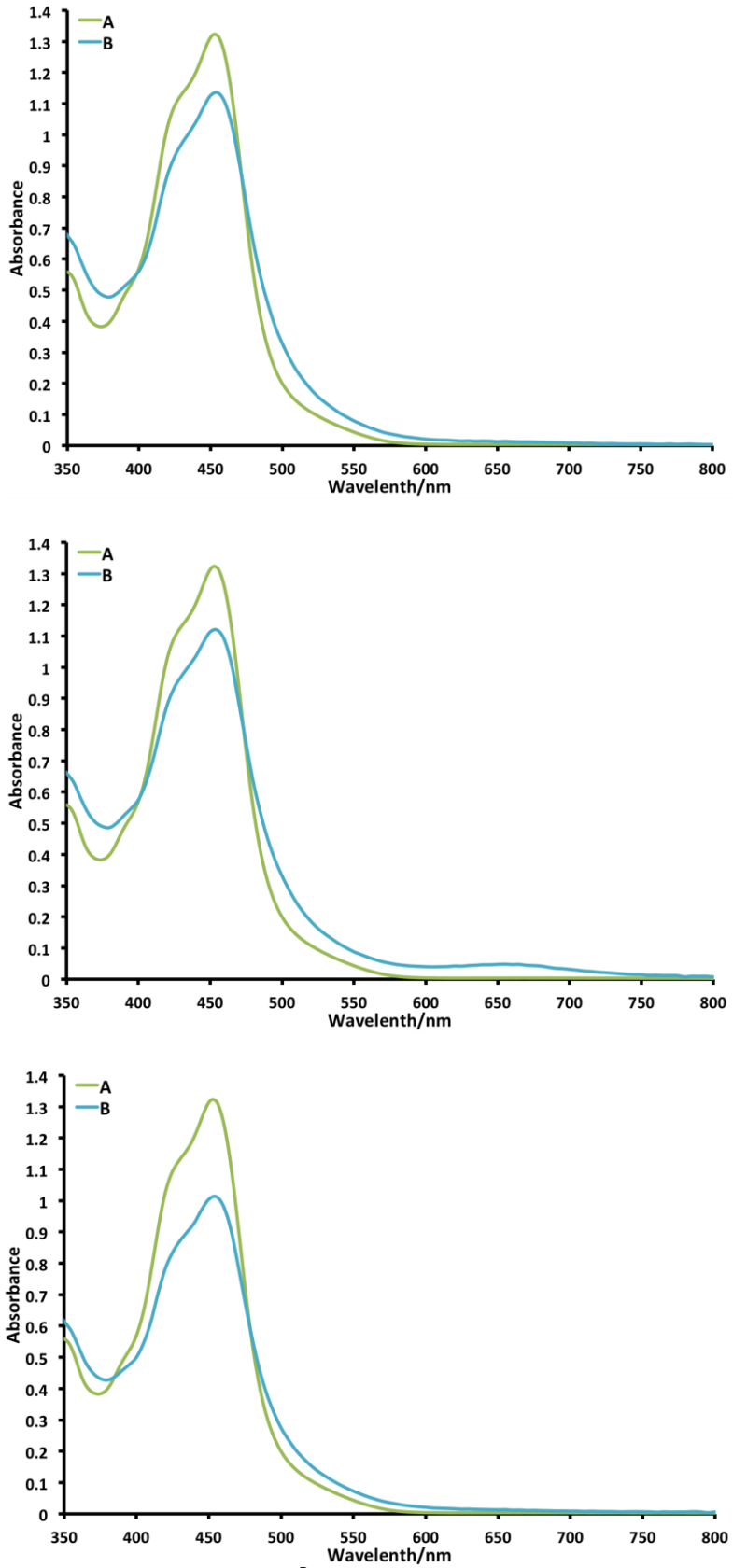

Figure S11. UV-Vis absorption of $Ru(bpy)_3^{2+}$ freshly prepared reaction solution before illumination (A, green traces), compared with that after catalysis (B, blue traces) for **Co$_9$** (top), **Co$_{15}$** (middle) and **Co$_{16}$** (bottom). Conditions: total cobalt concentration [**Co**]$_T$ = 147 µM, [$Ru(bpy)_3^{2+}$] = 1 mM, [$Na_2S_2O_8$] = 5 mM in 20 mM phosphate buffer, pH 8.

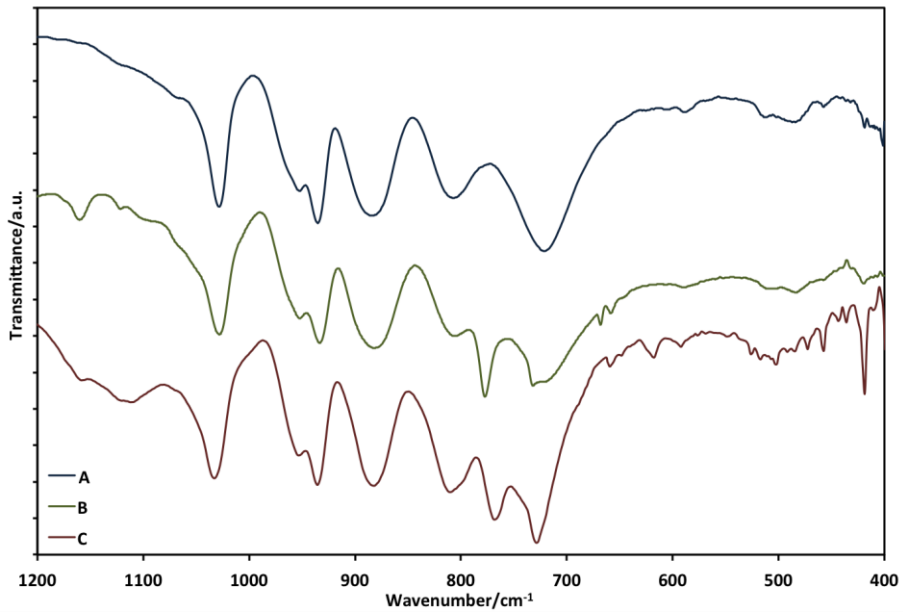

Figure S12. FTIR spectra of pristine **Co$_9$** (A; blue), adduct of **Co$_9$**·Ru(bpy)$_3^{2+}$ after conductometric titration (B; green), and precipitate retrieved after water-oxidation reaction (C; red).

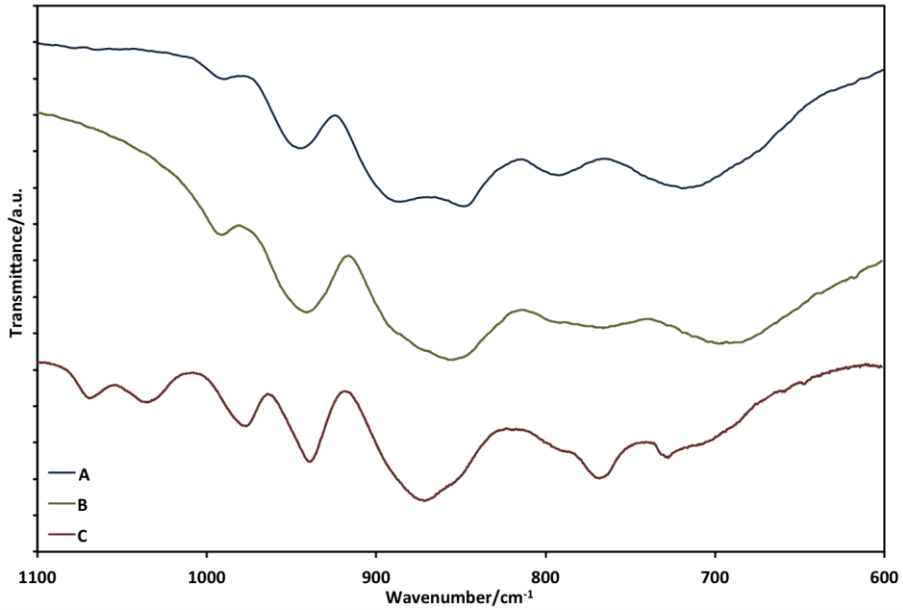

Figure S13. FTIR spectra of pristine **Co$_{15}$** (A; blue), adduct of **Co$_{15}$**·Ru(bpy)$_3^{2+}$ after conductometric titration (B; green), and precipitate retrieved after water-oxidation reaction (C; red).

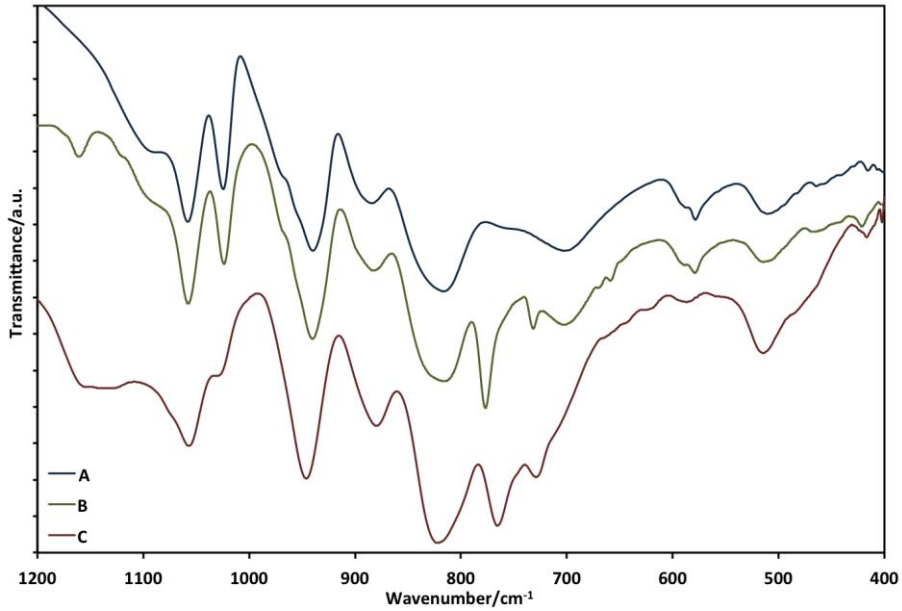

Figure S14. FTIR spectra of pristine **Co$_{16}$** (A; blue), adduct of **Co$_{16}$**·Ru(bpy)$_3^{2+}$ after conductimetric titration (B; green), and precipitate retrieved after water-oxidation reaction (C; red).

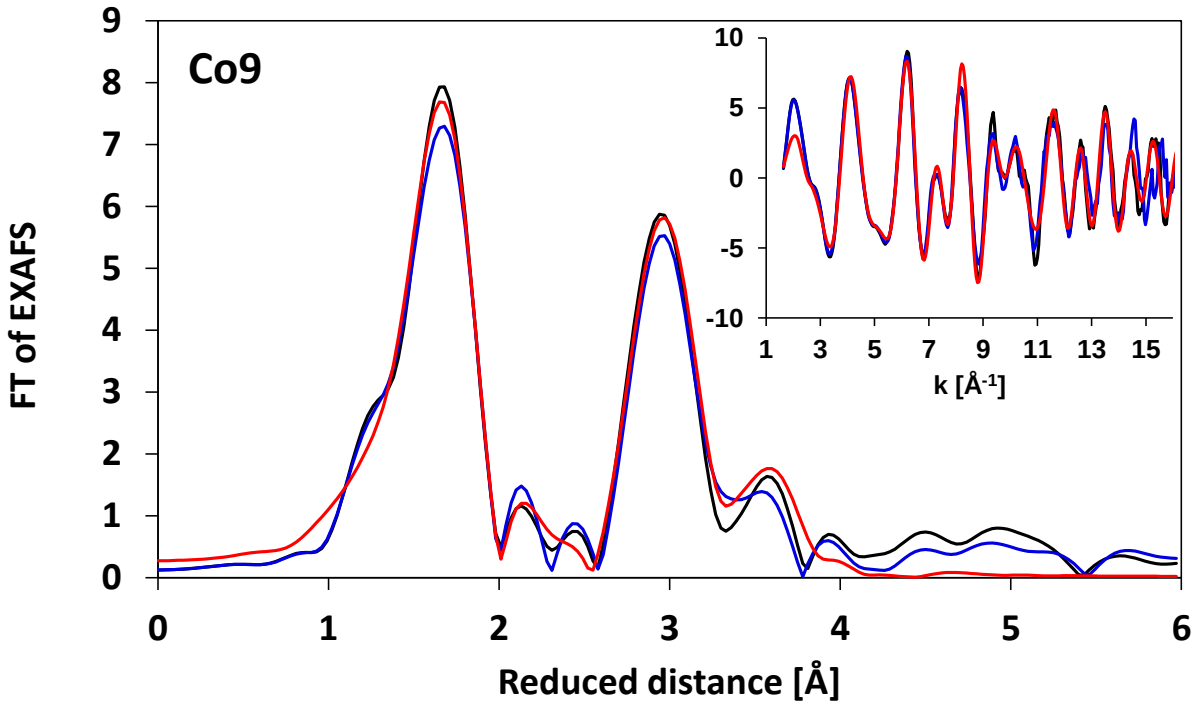
Co9
FT of EXAFS
Reduced distance [Å]
k [Å-1]

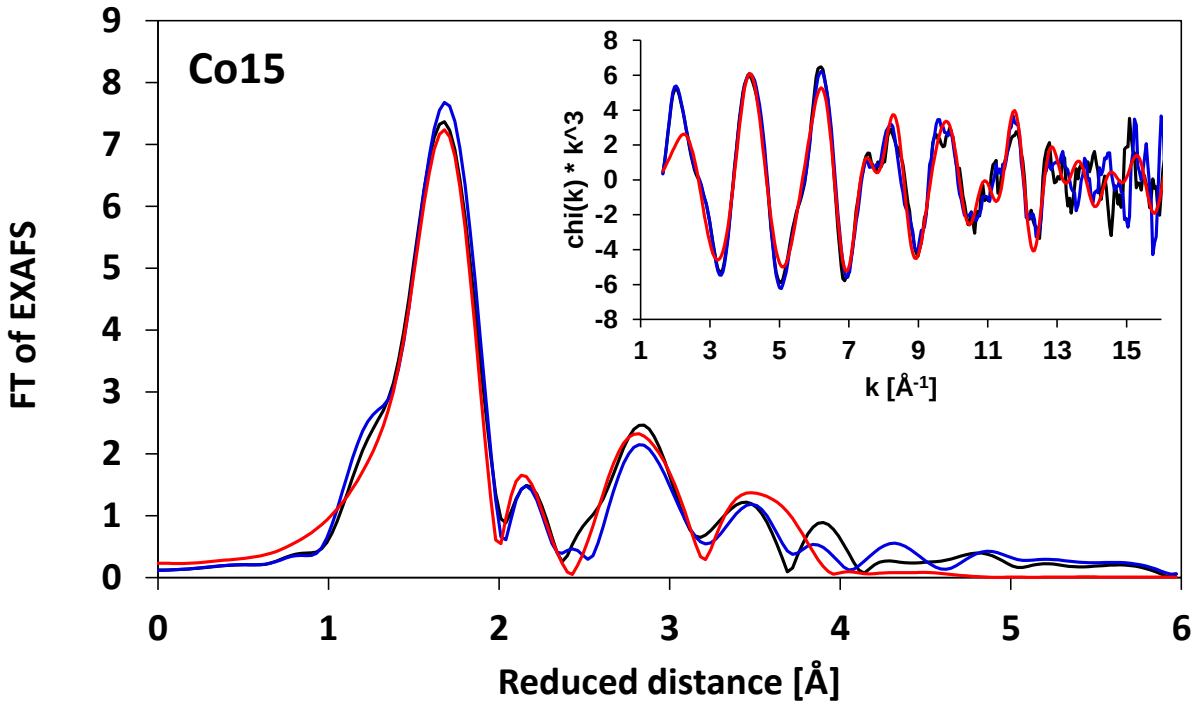
Co15
FT of EXAFS
Reduced distance [Å]
chi(k) * k^3
k [Å-1]

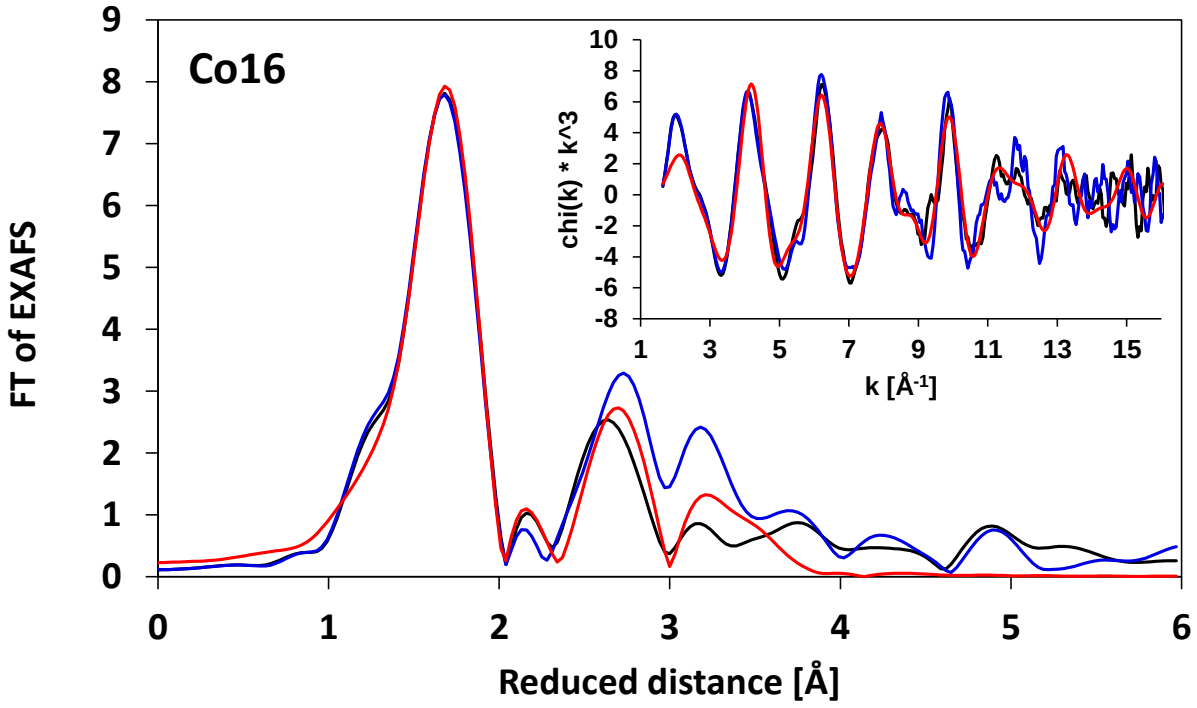

Figure S15. Fourier transformed experimental EXAFS of Co-POMs (black traces) and of their adduct with $Ru(bpy)_3^{2+}$ (bue traces). Fourier transforms were obtained in *k*-range 1.6 to 16.4 $Å^{-1}$ applying cosine window function extended over 10% at the beginning and 50% at the end of the experimental data. In red the Fourier transform of the simulated spectrum is shown. The simulation is done minimizing the difference between the spectrum of the pristine Co-POM (black line) and the calculated spectrum (in red). The simulation parameters are shown in Table S1. Insets: data in *k*-space.

Table S1. Simulation parameters obtained by minimization of the differences between the pristine CoPOM powders and the simulated spectrum in *k*-space. For simulation were used k^3-weighted experimental spectra in the range 1.6 to 16.4 $Å^{-1}$. The errors (grey color) represent the 68% confidence interval of the respective fit parameter (R, absorber-backscatter distance; σ, Debye-Waller parameter). The coordination numbers (N) were calculated according to the crystal structures and kept fixed during the simulation. For comparison the corresponding for each shell interatomic distances (according to the XRD structure) are shown in blue.

Co9

	Co-O	Co-Co	Co-P	Co-Co	Co-W	Co-O
N, XRD	6*	2*	2.3*	1.3*	2*	8.7*
R [Å], XRD	2.10	3.21	3.28	3.54	3.63	3.69
R [Å]	2.05	3.17	3.36	3.37	3.66	3.50
error	0.01	0.03	0.09	0.18	0.01	0.06
σ [Å]	0.067	0.061	0.032	0.053	0.054	0.067
error	0.001	0.004	0.021	0.018	0.002	0.001

Co15

	Co-O	Co-Cl	Co-Co	Co-Si	Co-W
N, XRD	5.6*	0.4*	1.2*	0.4*	2*
R [Å], XRD	2.09	3.46	3.11	3.19	3.67
R [Å]	2.06	2.46	3.11	3.22	3.63
error	<0.01	0.03	0.01	0.04	0.01
σ [Å]	0.067	0.067	0.060	0.032	0.067
error	0.003	0.023	0.011	0.038	0.004

Co16

	Co-O	Co-Co	Co-P	Co-Co	Co-W	Co-O
N, XRD	6*	2.3*	1.5*	1.5*	1.5*	3.3*
R [Å], XRD	2.12	3.03	3.19	3.78	3.33	3.53
R [Å]	2.06	3.02	3.04	3.70	3.33	3.48
error	0.01	0.14	0.18	0.05	0.38	0.14
σ [Å]	0.063	0.067	0.054	0.067	0.067	0.032
Error	0.005	0.001	0.160	0.002	0.067	0.160

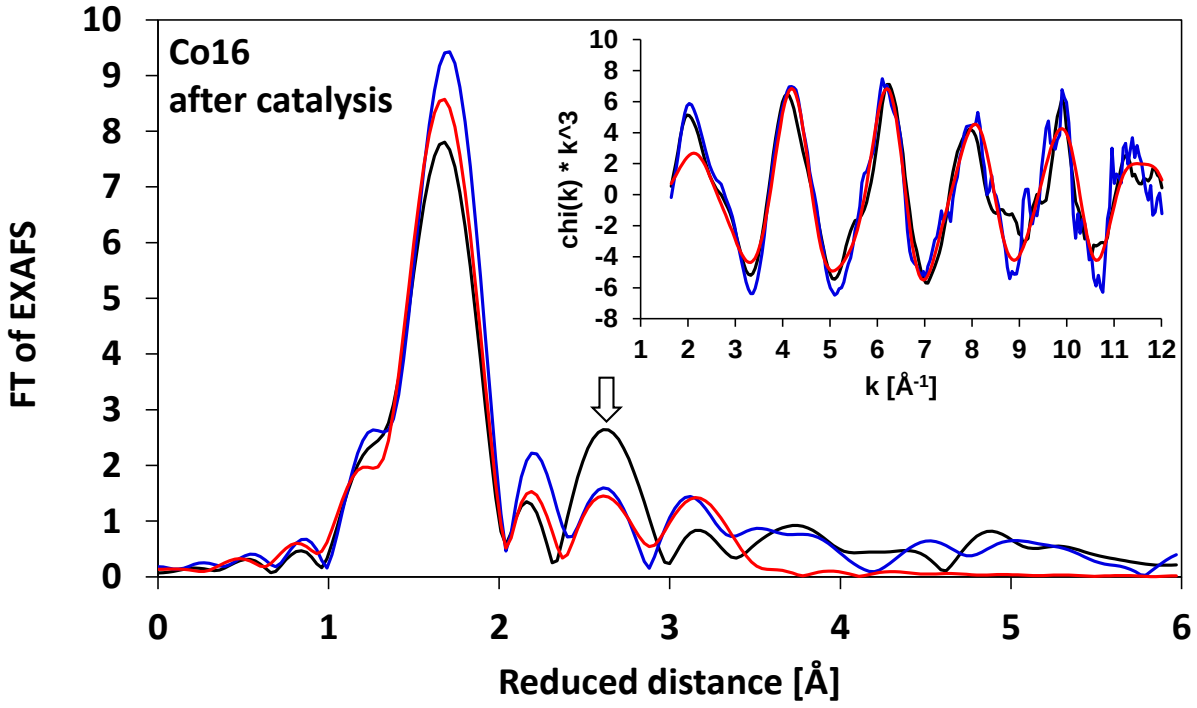

Figure S16. Fourier transformed experimental EXAFS for Co16 pristine powder (black trace) and for the used reaction mixture (blue trace). Fourier transforms were obtained in *k*-range 1.6 to 12.0 $Å^{-1}$ applying cosine window function extended over 10% at the beginning and at the end of the experimental data. In red the Fourier transform of the simulated spectrum of the used reaction mixture. The simulation parameters are shown in Table S2. Insets: data in *k*-space. The arrow indicates the lowering of the second peak amplitude related to decreased number of Co-Co vectors.

Table S2. Simulation parameters obtained for the EXAFS spectrum of the used reaction mixture For simulation were used k^3-weighted experimental spectra in the range 1.6 to 12.0 $Å^{-1}$. The distances (R) and the Debye-Waller factors (σ) were fixed to their values obtained for the pristine **Co_{16}** crystalline powder (Table 1) and only the coordination numbers (N) were varied during the simulation. Red color: an additional Co-Co distance of 2.81 Å typical for the catalytically active Co oxides (M. Risch, V. Khare, I. Zaharieva, L. Gerencser, P. Chernev, H. Dau, *J. Am. Chem. Soc.* 2009, **131,** 6936) was used but could not be resolved in the simulation (coordination number clearly below 0.1). The errors (grey color) represent the 68% confidence interval. For comparison the corresponding for each shell coordination numbers (according to the XRD structure) are shown in blue.

	Co16 after catalysis						
	Co-O	**Co-Co**	**Co-P**	**Co-Co**	**Co-W**	**Co-O**	**Co-Co (2.81 Å)**
R [Å], XRD	2.12	3.03	3.19	3.78	3.33	3.53	
N, XRD	6	2.3	1.5	1.5	1.5	3.3	
N	6.0	0.9	0.3	0.2	1.5	4.0	< 0.1
Error	0.1	0.6	0.7	0.6	0.6	1.3	0.3

Table S3. Turnover number (TON) and turnover frequencies for Cobalt polyoxometalates in photo-assisted oxygen production with /$Ru(bpy)_3^{2+}$ / $Na_2S_2O_8$ system.

#	Co-POM	Conditions and Light source	TON	TOF (s^{-1})	Ref
1	$[Co_4(H_2O)_2(\alpha\text{-}PW_9O_{34})_2]^{10-}$	Phosphate buffer, pH 8, irrad. 420-470 nm	220	≈ 0.8	[1]
2	$[Co_4(H_2O)_2(\alpha\text{-}VW_9O_{34})_2]^{10-}$	80 mM borate buffer, pH 9, irrad. 455 nm.	750	≈ 4	[2]
3	$[\{Co_4(OH)_3(PO_4)\}_4(XW_9O_{34})_4]^{n-}$ (X=Si, Ge, n=32 ; X = P, As, n =28).	80 mM borate buffer, pH 9, irrad. 300 W Xe lamp, 320 – 800 nm.	44-72	0.05 – 0.1	[3]
4	$[CoMo_6O_{24}H_6]^{3-}$ and $[Co_2Mo_{10}O_{38}H_4]^{6-}$,	100 mM borate buffer, pH 8, irrad. 300 W Xe lamp, 400 – 800 nm.	107-152	0.11-0.16	[4]
5	$[Co^{III}Co^{II}(H_2O)W_{11}O_{39}]^{7-}$	Borate buffer, pH 9, irrad > 420 nm	360	0.5	[5]

Table S4. Quantum yield (QY) values for photo-assisted oxygen production using a three component catalyst /$Ru(bpy)_3^{2+}$ / $Na_2S_2O_8$ sacrificial system. QY is defined as the ratio between the amount of O_2 formed and the photons absorbed by the system; in such photocatalytic cycle the maximum theoretical value for QY is 0.50.[6]

#	catalyst	Conditions and Light source	QY	Ref
1	$\{Ru_4O_4(\mu\text{-}OH)_2(H_2O)_4[\gamma\text{-}SiW_{10}O_{36}]\}^{10-}$	Phoshate buffer, pH 7.2, irrad. 420-550 nm	0.045	[7]
2	$\{Ru_4O_4(\mu\text{-}OH)_2(H_2O)_4[\gamma\text{-}SiW_{10}O_{36}]\}^{10-}$	Na_2SiF_6/$NaHCO_3$, pH 5.8, irrad. 420-550 nm	0.07	[8]
3	$[Co_4(H_2O)_2(\alpha\text{-}PW_9O_{34})_2]^{10-}$	Phosphate buffer, pH 8, irrad. 420-470 nm	0.15	[1]
4	$[Co_4(H_2O)_2(\alpha\text{-}VW_9O_{34})_2]^{10-}$	Borate buffer, pH 9, irrad. 455 nm.	0.34	[2]
5	$[Co^{III}Co^{II}(H_2O)W_{11}O_{39}]^{7-}$	Borate buffer, pH 9, irrad > 420 nm	0.27	[5]
6	Co(II)	Borate buffer, pH 8, irrad. 450 nm (1.58×10^{-7} einstein·s^{-1})	0.11	[9]
7	Co_3O_4 / SBA	Na_2SiF_6/$NaHCO_3$, pH 5.8, irrad. 476 nm	0.09	[10]

References

[1] Z. Huang, Z. Luo, Y. V. Geletii, J. W. Vickers, Q. Yin, D. Wu, Y. Hou, Y. Ding, J. Song, D. G. Musaev, C. L. Hill and T. Lian, *J. Am. Chem. Soc.*, 2011, **133**, 2068.

[2] H. Lv, J. Song, Y. V. Geletii, J. W. Vickers, J. M. Sumliner, D. G. Musaev, P. Kögerler, P. F. Zhuk, J. Bacsa, G. Zhu and C. L. Hill, *J. Am. Chem. Soc.* 2014, **136**, 9268.

[3] X.-B. Han, Z.-M. Zhang, T. Zhang, Y.-G. Li, W. Lin, W. You, Z.-M. Su and E.-B. Wang, *J. Am. Chem. Soc.* 2014, **136**, 5359.

[4] S. Tanaka, M. Annaka and K. Sakai, *Chem. Commun.* 2012, **48**, 1653.

[5] F. Song, Y. Ding, B. Ma, C. Wang, Q. Wang, X. Du, S. Fu and J. Song, *Energy Environ. Sci.* 2013, **6**, 1170.

[6] A. Sartorel, M. Bonchio, S. Campagna and F. Scandola *Chem. Soc. Rev.*, 2013, **42**, 2262.

[7] Y. V. Geletii, Z. Huang, Y. Hou, D. G. Musaev, T. Lan and C. L. Hill, *J. Am. Chem. Soc.*, 2009, **131**, 7522.

[8] C. Besson, Z. Huang, Y. V. Geletii, S. Lense, K. I. Hardcastle, D. G. Musaev, T. Lian, A. Proust and C. L. Hill, *Chem. Commun.*, 2010, **46**, 2784.

[9] A. Genoni, G. La Ganga, A. Volpe, F. Puntoriero, M. Di Valentin, M. Bonchio, M. Natali and A. Sartorel, *Faraday Disc.* 2015, **185**, 121.

[10] F. Jiao and H. Frei, *Angew. Chem., Int. Ed.*, 2009, **48**, 1841.